Defect-Mediated Island Formation in Stranski-Krastanov Growth of Ge on Si(001)

Akira Sakai and Toru Tatsumi
Microelectronics Research Laboratories, NEC Corporation, 34 Miyukigaoka, Tsukuba, Ibaraki 305, Japan
(Received 30 July 1993)

We have observed macroscopic island (macroisland) formation in Stranski-Krastanov growth of Ge on Si(001) surfaces under various growth conditions using transmission electron microscopy. The interplay between surface morphological evolution and defect formation during growth was revealed. We show that the nucleation of macroislands is predominantly heterogeneous. Furthermore, evidence is presented that macroisland formation is mediated by a particular defect which results from the coalescence of small faceted islands.

PACS numbers: 68.35.Bs, 68.55.Ln

Investigation of Ge growth on Si is fundamental both for understanding essential mechanisms in strain-related heteroepitaxial growth and for fabricating high quality SiGe/Si and Ge/Si heterostructures for optoelectronic devices. It is well-known that Stranski-Krastanov growth occurs in the growth of Ge on Si substrates. Extensive studies have been done revealing the early stages of Ge growth on Si(001) surfaces [1-8]. It was recently reported that before the onset of macroscopic island (macroisland) formation, small islands, so-called *hut clusters*, were formed on the surface [1,2]. These hut clusters had four {501} facet planes and were strictly aligned along the two orthogonal ⟨100⟩ directions of the substrate. On the other hand, it has also been reported that nonfaceted, dislocation-free islands can be formed at almost the same stage of growth [4]. Strain relaxation would then have to be accomplished by local elastic deformation of near-surface layers in the substrate. This implies that the primary driving force for island formation is not the ability to introduce dislocations but rather strain energy reduction by forming island morphology itself on the surface [4-6]. Further Ge deposition leads to formation of macroislands with mostly {311} facet planes [8].

In this study, we concentrate on the growth stage of the macroisland of Ge on the Si(001) surface. A mechanism for its formation has been proposed [1], but clear experimental evidence was lacking until now. Although a systematic study addressing the initial stage of islanding has been recently reported [5], open questions have included the nature of the nucleation stage of macroisland formation, i.e., whether it is homogeneous or heterogeneous, and how this relates to defect formation. In particular, as mentioned above, Ge growth on Si proceeds in a complicated manner in which morphological variations of the surface are closely related to strain relief of the evolving film. Thus experimental tools are required which can simultaneously detect both surface morphological evolution and defect structures inside the film and/or at the Ge/Si interface. In this paper we have carried out plan-view transmission electron microscopy (TEM) and cross-sectional high-resolution (HR) TEM for Ge/Si structures prepared under various growth conditions in order to investigate the formation mechanism of the macroislands. We found for the first time that the nucleation of macroislands on a surface having initially small faceted islands is heterogeneous. We also present evidence that macroisland formation is mediated by a particular defect which lies along a specific direction with respect to the faceted island.

Ge growth on Si(001) substrates was performed using ultrahigh vacuum solid-source molecular beam epitaxy (MBE) equipment with a base pressure of 1×10^{-10} Torr. The Si source was an 8 kV electron beam evaporator and Ge was deposited from a boron nitride Knudsen cell. After cleaning the substrate surface [9], a 1000 Å thick buffer layer was grown, which showed a 2×1 reconstruction. Ge was then deposited at a rate of 0.02 monolayer (ML)/sec at a particular substrate temperature. The pressure rose to no more than 10^{-8} Torr during deposition. No surface contaminants were detected by *in situ* Auger electron spectroscopy. Surface structures were monitored during Ge deposition by *in situ* reflection high energy electron diffraction. Samples prepared under various growth conditions were mechanically and chemically thinned from the substrate side for plan-view TEM observations and Ar ion milled for ⟨110⟩ cross-sectional observations. TEM was performed with a TOPCON EM-002B operating at 200 kV.

Figure 1(a) shows a typical plan-view bright-field image of a sample in which 7 ML Ge was deposited at a substrate temperature of 300 °C. The image was taken with a defocus value of −9000 Å under conventional nontilted imaging conditions. Small rectangular and square-shaped structures are clearly observed. By taking images of the same area with several defocus values, it was confirmed that this image reflected the morphology existing on only one side of the TEM specimen, where the Ge growth was performed. From their size and alignment strictly along the two ⟨100⟩ directions of the substrate we identify these as the hut clusters (faceted islands) previously observed by scanning tunneling microscopy [1,2]. Figure 1(b) is the corresponding transmission electron diffraction (TED) pattern. Note that extra spots elongated along the ⟨110⟩ directions of the substrate, indicated by arrowheads *A* and *B*, can be observed near the positions corresponding to a {111} lattice spacing. As

0031-9007/93/71(24)/4007(4)$06.00

© 1993 The American Physical Society

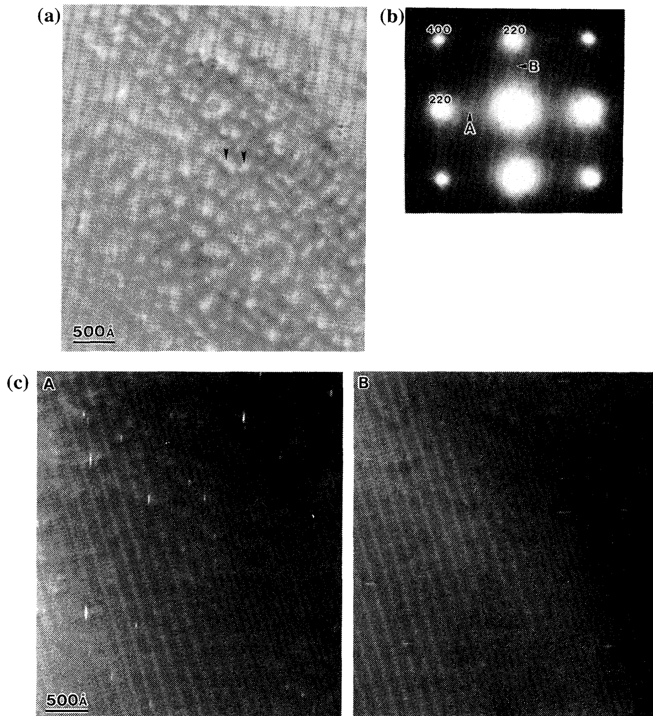

FIG. 1. (a) Plan-view bright-field TEM micrograph of a sample with 7 ML Ge grown on a Si(001) substrate showing faceted islands strictly aligned along two orthogonal ⟨100⟩ directions. (b) Corresponding TED pattern showing two types of extra spots elongated along ⟨110⟩ directions, indicated by the arrowheads A and B. (c) Plan-view dark-field TEM micrographs of the same are observed in (a), take with the "A" and "B" extra spots in (b).

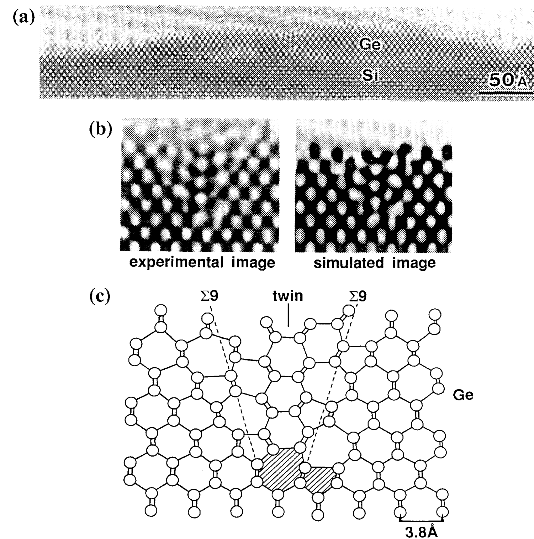

FIG. 2. (a) Cross-sectional HRTEM micrograph of the sample of Fig. 1 in the ⟨110⟩ projection. Note the V-shaped defect between two faceted islands. (b) Comparison between the experimental image and the simulated image obtained from the atomic model of (c). (c) Atomic model of the defect projected in the ⟨110⟩ direction. The shaded region at the cusp of the defect shows a pair of five- and seven-membered atomic rings.

shown in Fig. 1(c), dark-field images made with the respective extra spots exhibit defects running along the ⟨110⟩ direction perpendicular to the elongation direction of the spot in the TED pattern. These results demonstrate correlation of surface microscopic island morphology with the distribution of defects inside the film; careful comparison between the bright-field and the dark-field images explicitly shows that the defects are situated where the faceted islands coalesce. For example, the defect denoted by D in Fig. 1(c) is observed between two faceted islands indicated by arrowheads in Fig. 1(a). By both wide-range observations and measurements at various specimen tilt angles, we also confirmed that this was the only type of defect present.

A cross-sectional HRTEM image of the same sample is shown in Fig. 2(a). A defect is clearly observed between two faceted islands. The atomic structure of the defect was examined using a multislice image simulation [10]. Figure 2(b) compares the experimental image with the simulated image obtained from the most probable atomic model, shown in Fig. 2(c). The defect has a twin structure with a ⟨211⟩ surface normal at the center and the twin region is separated from the matrix by two Σ9 grain boundaries, forming a V shape. Thus the appearance of the extra spot near the {111} spacing in the TED pattern can be immediately understood as due to the {111} lattice planes which the defect contains parallel to {110} lattice planes of the substrate. Note that the structure of the defect, hereafter called T-Σ9D, is quite similar to one previously observed in Ge films on Si(001) substrates prepared by surfactant epitaxy [11]. However, to our knowledge, this is the first observation of T-Σ9D's formed during conventional MBE growth of Ge on Si.

A previous report claimed that formation of the T-Σ9D was due to a specific growth process, i.e., a forced layer-by-layer growth manner mediated by surfactants [11]. However, the fact that we observed this defect in a film prepared by conventional MBE clearly indicates that its formation is due to an intrinsic process of Ge growth on the Si(001) surface. Although the formation energy of T-Σ9D is comparable to that of an edge dislocation [12], it seems unlikely that it is extrinsically introduced from the surface like a misfit dislocation since the formation process requires considerable bond rearrangement in the film. This idea is also supported by the observation that layer-by-layer growth induced by low-temperature deposition did not lead to the introduction of T-Σ9D but rather to dislocations [13].

We note here some significant features of T-Σ9D observed under various growth conditions. First, the T-Σ9D was always formed on faceted islands. As shown later, in the case of growth at temperatures higher than ~600 °C where nonfaceted islands are dominant, no T-Σ9D's were

observed at any stages of growth. These results suggest that T-$\Sigma 9D$ formation is closely related to the manner of growth of the faceted islands. Second, we confirmed a dependence of the number density of T-$\Sigma 9D$'s on the number density and average size of the faceted islands. It was observed that lower temperature growth led to the formation of faceted islands having a higher number density but a smaller average size, while higher temperature growth had the opposite effect, even though the deposited amounts of Ge were equivalent. This resulted in the formation of a higher number density of T-$\Sigma 9D$'s for lower temperature growth. Third, we point out again the specific formation site of T-$\Sigma 9D$'s between two faceted islands as confirmed in Figs. 1 and 2(a). All these features strongly suggest the nature of T-$\Sigma 9D$ as a *grown-in* defect during film evolution.

Following this idea, notice that the pair of five-membered and seven-membered atomic rings ($P5$-$7AR$) at the cusp of T-$\Sigma 9D$, seen as the shaded zone in Fig. 2(c), must nucleate at the first stage of defect formation. What causes the nucleation of $P5$-$7AR$? We believe that the low reactivity with the incoming Ge atoms of the dimer bond in the surface dimer structure, which is essentially identical to the five-membered atomic ring, accelerates the nucleation of $P5$-$7AR$ during growth. It has been demonstrated that the domain compressed along the dimer bond was favored under an externally applied stress [14]. Theoretical studies also reported that dimerization of the (001) surface atoms caused a tensile stress parallel to the dimer bond [15]. Thus it is reasonable to interpret that the compressive stress applied to the Ge film by the lattice mismatch between Ge and Si stabilizes the surface dimers on the faceted island compared with the nonstrained systems. Furthermore, single-stepped surfaces having zigzag dimer structures have been observed on the faceted islands [1,2]. This result implies that not only the dimer but also the single-stepped morphology contributes to stress compensation. Therefore, it seems likely that more compressive stress, compared with the other regions, is accumulated at the sites where coalescence of the faceted islands occurs, since a combination of two orthogonal $\langle 100 \rangle$ steps on the two faceted islands directly means a loss of the step contribution to stress compensation. In view of this, the dimer bond at the coalescence site is expected to be less reactive, preserving five-membered atomic ring structure during growth; this gives rise to the reduction of the nucleation barrier for $P5$-$7AR$ formation. Once $P5$-$7AR$ nucleates on the growth surface, diffusing atoms are automatically incorporated easily forming twin and $\Sigma 9$ boundary structures on it, since the $\Sigma 9$ boundary also consists of chained $P5$-$7AR$'s.

Next we will report on macroisland formation. Further deposition of Ge led to the onset of macroisland formation on the faceted islands. In Fig. 3(a), a bright-field image of a sample with 12 ML of Ge shows macroislands exhibiting moiré fringes as well as smaller faceted islands.

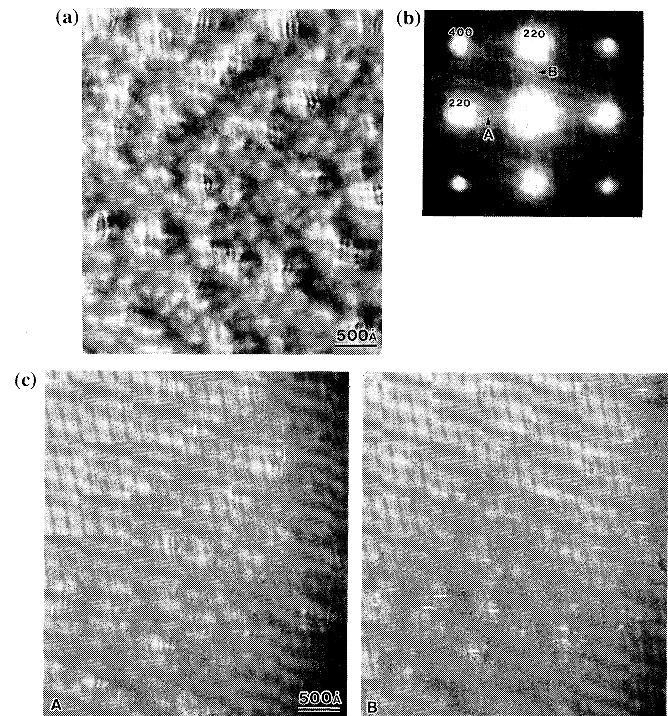

FIG. 3. (a) Plan-view bright-field TEM micrograph of a sample with 12 ML Ge grown on a Si(001) substrate. Macroisland images showing moiré fringes as well as faceted islands can be observed. (b) TED pattern corresponding to the image of (a). Note that the intensity of the extra spots is increased compared with Fig. 1(b). (c) Plan-view dark-field TEM micrographs of the same area observed in (a), taken in the same manner as Fig. 1(c). Note that all defect images overlap with the moiré fringes of the macroislands.

In the corresponding TED pattern shown in Fig. 3(b), the intensity of the extra spots caused by T-$\Sigma 9D$'s are observed to increase compared with that of the sample shown in Fig. 1(b). Dark-field images of the corresponding region are shown in Fig. 3(c), which were taken in the same manner as in Fig. 1(c). The number density of the defects in both images is significantly higher than in Fig. 1(c). Comparing bright-field and dark-field images, the most remarkable feature is that there is a one-to-one correspondence between the macroislands and the defects. Some macroislands contain defects along both orthogonal $\langle 110 \rangle$ directions while others contain only defects along one direction. Figure 4 is a typical cross-sectional HRTEM image of the same sample. It is clearly observed that a T-$\Sigma 9D$ is buried in the macroisland but the twin and $\Sigma 9$ boundary structure is still preserved. These results unambiguously indicate that the macroislands prefer to grow in the vicinity of a T-$\Sigma 9D$, meaning that nucleation for macroisland formation is predominantly heterogeneous. We found that this heterogeneity is dominant at the substrate temperatures, T, up to $\sim 450\,°C$. However, for $T > \sim 550\,°C$, the nucleation

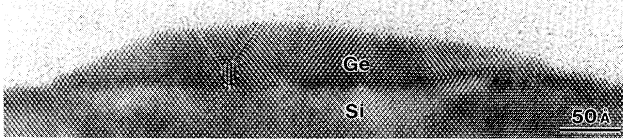

FIG. 4. Cross-sectional HRTEM micrograph showing a macroisland in the ⟨110⟩ projection. Note T-$\Sigma 9D$ with new microtwins generated in the macroisland.

becomes homogeneous. In this high temperature case, by depositing increasing amounts of Ge, nonfaceted, initially dislocation-free islands with a lower number density than that of the faceted islands were continuously grown without the T-$\Sigma 9D$ formation. After a certain amount of Ge was deposited, misfit dislocations were introduced into the island resulting in complete strain relaxation, as has been previously reported [4].

How can we explain this dependence on the growth temperature of the manner of nucleation for macroisland formation? In general, dominance of either a homogeneous or a heterogeneous manner in the nucleation stage of a system is determined by two principal factors: the driving force for nucleation and the interface energy caused by formation of a new phase in a matrix phase [16]. In the case of macroisland formation in the Ge/Si system, the interace energy, i.e., the surface energy of the macroisland, varies little with the growth temperature since the morphology of macroislands formed at various growth temperatures is almost the same. Therefore, dominance of the nucleation manner should be explained in consideration of the driving force and its kinetic limitation. At high temperatures, with less kinetic limitation, a simple growth process occurs in which an initially small dislocation-free, nonfaceted island develops into a larger macroisland. Thus the nucleation is homogeneous. On the other hand, it has been reported that island formation is greatly suppressed by low-temperature growth [13,17]. This result strongly suggests that lowering the growth temperature kinetically limits the driving force for macroisland formation. In this situation, the system might be driven into T-$\Sigma 9D$ formation on the faceted island, instead of direct formation of the macroisland on the surface. The T-$\Sigma 9D$ primarily plays two important roles for further Ge growth. First, it contributes to partial strain energy release of the evolving film before macroisland formation. Since a T-$\Sigma 9D$ has close-packed {111} planes parallel to the {110} plane of the substrate and a V-shaped morphology from introducing two $\Sigma 9$ boundaries, the compressive stress due to lattice mismatch is gradually relaxed as the film grows [11]. Second, it directly mediates macroisland formation by acting as a preferential nucleation site. It is well known that the energy barrier for nucleation is reduced by the free energy of a defect [18]. Thus macroisland formation easily proceeds in a heterogeneous nucleation manner, even with the kinetically limited driving force, so as to decrease the extra free energy created by the defect.

From a kinetic point of view, preferential growth in the vicinity of a T-$\Sigma 9D$ can be explained on the consideration that the defect is at a site where two orthogonal steps combine; this site acts as a stronger sink for surface diffusive Ge atoms than the other steps of the faceted islands. Furthermore, diffusing atoms may be easily trapped by extra dangling bonds on the surface of a T-$\Sigma 9D$. Thus the growth rate around the defect will be increased, forming a macroisland.

The ideas mentioned above basically support the interpretation given by Mo *et al.*, that faceted island formation is the kinetic pathway for macroisland formation [1]. However, we emphasize here that macroisland formation is actually mediated by the formation of T-$\Sigma 9D$ which is due to the coalescence of the faceted islands.

[1] Y.-W. Mo *et al.*, Phys. Rev. Lett. **65**, 1020 (1990).
[2] F. Iwawaki, M. Tomitori, and O. Nishikawa, Surf. Sci. Lett. **253**, L411 (1991).
[3] U. Köhler *et al.*, Ultramicroscopy **42-44**, 832 (1992).
[4] D. J. Eaglesham and M. Cerullo, Phys. Rev. Lett. **64**, 1943 (1990).
[5] M. Krishnamurthy, J. S. Drucker, and J. A. Venables, J. Appl. Phys. **69**, 6461 (1991).
[6] P. Ashu and C. C. Matthai, Appl. Surf. Sci. **48/49**, 39 (1991).
[7] A. A. Williams *et al.*, Phys. Rev. B **43**, 5001 (1991).
[8] Y. Koide *et al.*, Jpn. J. Appl. Phys. **28**, 690 (1989).
[9] T. Tatsumi, N. Aizaki, and H. Tsuya, Jpn. J. Appl. Phys. **24**, L277 (1985).
[10] In the calculations, the following parameters were used: the specimen thickness, 70 Å; objective lens defocus value, −200 Å; spherical aberration, 0.4 mm; defocus spread, 64 Å; beam convergence, 0.85 mrad.
[11] F. K. LeGoues, M. Copel, and R. Tromp, Phys. Rev. Lett. **63**, 1826 (1989); Phys. Rev. B **42**, 11 690 (1990).
[12] R. E. Thomson and D. J. Chadi, Phys. Rev. B **29**, 889 (1984).
[13] D. J. Eaglesham and M. Cerullo, Appl. Phys. Lett. **58**, 2276 (1991).
[14] F. K. Men, W. E. Packard, and M. B. Webb, Phys. Rev. Lett. **61**, 2469 (1988); M. B. Webb *et al.*, J. Vac. Sci. Technol. A **8**, 2658 (1990).
[15] O. L. Alerhand *et al.*, Phys. Rev. Lett. **61**, 1973 (1988); R. D. Meade and D. Vanderbilt, in *Proceedings of the Twentieth International Conference on the Physics of Semiconductors*, edited by E. M. Anastassakis and J. D. Joannopoulos (World Scientific, Singapore, 1990), p. 123.
[16] R. D. Doherty, in *Physical Metallurgy*, edited by R. W. Cahn and P. Haasen (North-Holland, Amsterdam, 1983), p. 952.
[17] H.-J. Gossmann and L. C. Feldman, Surf. Sci. **155**, 413 (1985).
[18] J. W. Christian, in *The Theory of Transformation in Metals and Alloys I* (Pergamon, Oxford, 1981), p. 448.

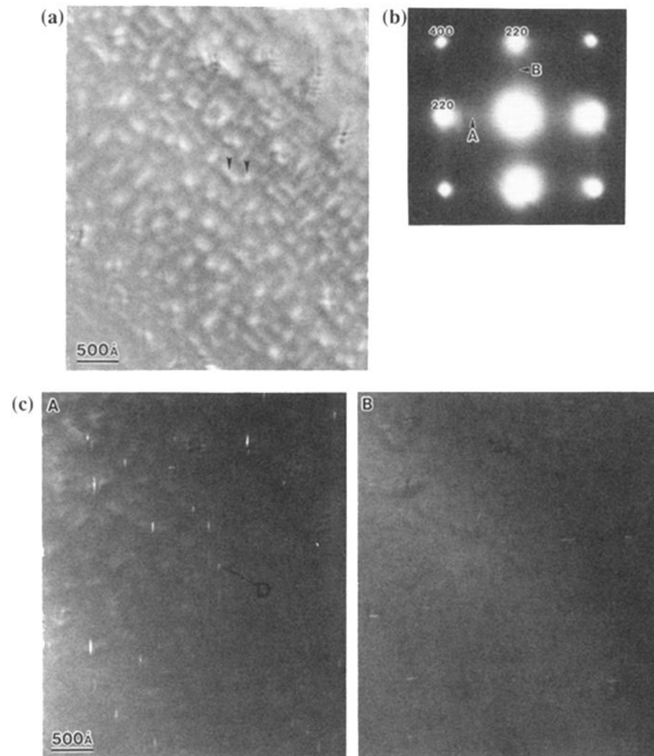

FIG. 1. (a) Plan-view bright-field TEM micrograph of a sample with 7 ML Ge grown on a Si(001) substrate showing faceted islands strictly aligned along two orthogonal ⟨100⟩ directions. (b) Corresponding TED pattern showing two types of extra spots elongated along ⟨110⟩ directions, indicated by the arrowheads *A* and *B*. (c) Plan-view dark-field TEM micrographs of the same are observed in (a), take with the "*A*" and "*B*" extra spots in (b).

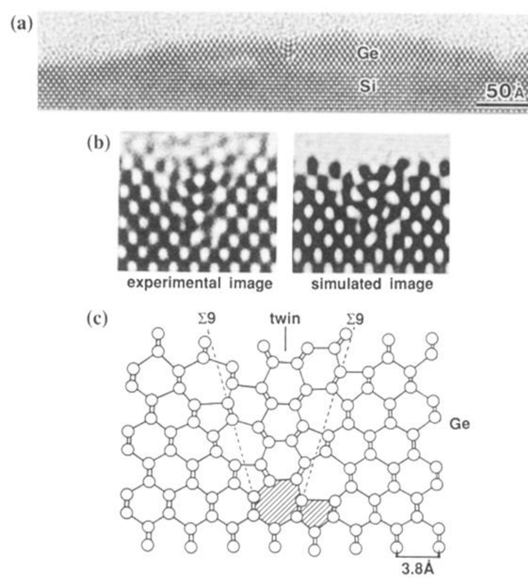

FIG. 2. (a) Cross-sectional HRTEM micrograph of the sample of Fig. 1 in the ⟨110⟩ projection. Note the V-shaped defect between two faceted islands. (b) Comparison between the experimental image and the simulated image obtained from the atomic model of (c). (c) Atomic model of the defect projected in the ⟨110⟩ direction. The shaded region at the cusp of the defect shows a pair of five- and seven-membered atomic rings.

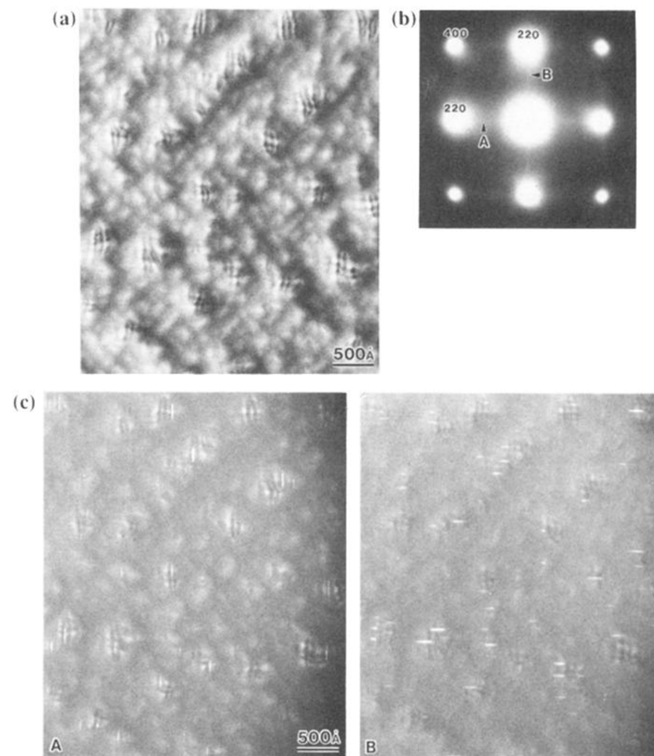

FIG. 3. (a) Plan-view bright-field TEM micrograph of a sample with 12 ML Ge grown on a Si(001) substrate. Macroisland images showing moiré fringes as well as faceted islands can be observed. (b) TED pattern corresponding to the image of (a). Note that the intensity of the extra spots is increased compared with Fig. 1(b). (c) Plan-view dark-field TEM micrographs of the same area observed in (a), taken in the same manner as Fig. 1(c). Note that all defect images overlap with the moiré fringes of the macroislands.

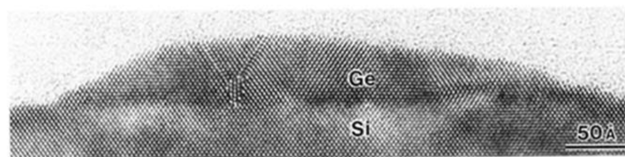

FIG. 4. Cross-sectional HRTEM micrograph showing a macroisland in the ⟨110⟩ projection. Note T-$\Sigma 9D$ with new microtwins generated in the macroisland.